Fujikawa, K., & McMullen, B. A. (1983) *J. Biol. Chem.* (in press).
Fujikawa, K., Legaz, M. E., & Davie, E. W. (1972) *Biochemistry 11*, 4882–4891.
Graves, C. B., Munns, T. W., Willingham, A. K., & Strauss, A. W. (1982) *J. Biol. Chem. 257*, 13108–13113.
Hamilton, P. B. (1968) in *CRC Handbook of Biochemistry* (Sober, H. A., Ed.) pp B52–B54, Chemical Rubber Publishing Co., Cleveland, OH.
Hayashi, R. (1977) *Methods Enzymol. 47*, 84–93.
Hugli, T. E., & Moore, S. (1972) *J. Biol. Chem. 247*, 2328–2834.
Johnson, A. E., Esmon, N. L., Laue, T. M., & Esmon, C. T. (1983) *J. Biol. Chem.* (in press).
Katayama, K., Ericsson, L. H., Enfield, D. L., Walsh, K. A., Neurath, H., Davie, E. W., & Titani, K. (1979) *Proc. Natl. Acad. Sci. U.S.A. 76*, 4990–4994.
Kisiel, W., Ericsson, L. H., & Davie, E. W. (1976) *Biochemistry 15*, 4893–4900.
Kivirikko, K. I., & Myllylä, R. (1980) in *The Enzymology of Post-Translational Modification of Proteins* (Freedman, R. B., & Hawkins, H. C., Eds.) pp 53–104, Academic Press, New York.
Koide, A., Titani, K., Ericsson, L. H., Kumar, S., Neurath, H., & Walsh, K. A. (1978) *Biochemistry 17*, 5657–5672.
Kurachi, K., & Davie, E. W. (1982) *Proc. Natl. Acad. Sci. U.S.A. 79*, 6461–6464.
Kuwada, M., & Katayama, K. (1981) *Anal. Biochem. 117*, 259–265.
Leclercq, P. A., & Desiderio, D. L. (1971) *Anal. Lett. 4*, 305–316.
Mahoney, W. C., & Hermodson, M. A. (1980) *J. Biol. Chem. 255*, 11199–11203.
Mann, K. G. (1976) *Methods Enzymol. 45*, 123–156.
Mann, K. G., Elion, J., Butkowski, R. J., Downing, M., & Nesheim, M. E. (1981) *Methods Enzymol. 80*, 286–302.
McMullen, B., Kisiel, W., & Fujikawa, K. (1982) *Circulation 66*, II-71, Abstr.
Moore, S., & Stein, W. H. (1963) *Methods Enzymol. 6*, 819–831.
Morris, H. R. (1979) *Philos. Trans. R. Soc. London, Ser. A No. 293*, 39–51.
Nemerson, Y., & Furie, B. (1980) *CRC Crit. Review Biochem.* 45–85.
Okai, H., Imamura, N., & Izumiya, N. (1967) *Bull. Chem. Soc. Jpn. 40*, 2154–2159.
Pepper, D. S., & Prowse, C. (1977) *Thromb. Res. 11*, 687–692.
Tarr, G. E. (1982) in *Methods in Protein Sequence Analysis* (Elzinga, M., Ed.) pp 223–232, Humana Press, Clifton, NJ.
Tarr, G. E., Beecher, J. F., Bell, M., & McKea, D. J. (1978) *Anal. Biochem. 84*, 622–627.
Titani, K., Fujikawa, K., Enfield, D. L., Ericsson, L. H., Walsh, K. A., & Neurath, H. (1975) *Proc. Natl. Acad. Sci. U.S.A. 72*, 3082–3086.
Woods, K. R., & Wang, K.-T. (1967) *Biochim. Biophys. Acta 133*, 369–375.

Fluorescence Depolarization of Tryptophan Residues in Proteins: A Molecular Dynamics Study†

Toshiko Ichiye and Martin Karplus*

ABSTRACT: A molecular dynamics simulation of lysozyme is used to examine the fluorescence depolarization of tryptophan residues on the picosecond time scale. The calculated time dependence of fluorescence emission anisotropy for the six tryptophans in lysozyme exhibits a wide variety of motional behavior that should correspond to the range expected more generally for tryptophan residues in proteins. It is found that some tryptophans are highly mobile with a large fluorescence anisotropy decay on the picosecond time scale while others are essentially rigid due to the presence of the protein matrix. Further, it is demonstrated that correlations among the internal degrees of freedom (e.g., dihedral angles) play an important role in the observed decay behavior; this suggests that care has to be used in interpreting experimental results in terms of simple motional models. Because the available experimental time resolution is limited to the nanosecond time scale, only the effective zero-time anisotropy can be compared with the calculated values. The results suggest that the study of fluorescence depolarization with femtosecond lasers would provide new insights into the short time dynamics of amino acid side chains in proteins.

A knowledge of the internal dynamics of proteins is important for an understanding of the physical properties and biological function of these molecules (Karplus & McCammon, 1981). At present, an increasing variety of experimental and theoretical methods are being used to study these motions. Of particular interest are experimental methods that can supplement X-ray temperature factors, which provide data on the magnitude of the fluctuations but no information on their time scales. Both nuclear magnetic resonance (NMR) relaxation and fluorescence depolarization experiments are useful in this regard since they provide data on the internal motions of proteins in the picosecond to nanosecond range. The parameters of interest in both types of experiments are related to time correlation functions whose decay is determined by reorientation of certain vectors associated with the probe (i.e.,

† From the Department of Chemistry, Harvard University, Cambridge, Massachusetts 02138. *Received July 15, 1982; revised manuscript received February 28, 1983.* Supported in part by the National Science Foundation and the National Institutes of Health.

0006-2960/83/0422-2884$01.50/0

vectors between nuclei for NMR relaxation and transition moment vectors for fluorescence depolarization). Application of the results of a molecular dynamics simulation of the bovine pancreatic trypsin inhibitor (PTI) to the carbon-13 relaxation of protonated carbons has shown that the picosecond motional averaging of the C–H dipole vector can increase the NMR spin–lattice relaxation time (T_1) by 10–100% (Levy et al., 1981a). Experimental evidence for such effects has been found in a number of NMR experiments (Wittebort et al., 1979; Richarz et al., 1980; Ribeiro et al., 1980). However, because the contributions of various types of motions to the NMR relaxation rates depend on the Fourier transform of the appropriate correlation functions (Levy et al., 1981a,b), it is difficult to obtain a unique result from the measurements. In fact, most experimental estimates of the time scales and magnitudes of the motions depend on the particular choice of model used for their interpretation. Fluorescence depolarization, although more limited in the sense that few protein residues (e.g., tryptophans and tyrosines) can be studied with present techniques, has the distinct advantage that the measured quantity depends directly on the decay of the correlation function. In principle, femtosecond laser techniques (Martin et al., 1983) could be used to resolve picosecond decay behavior, but at present, the available measurements are limited to the subnanosecond time scale; e.g., in the study of Munro et al. (1979), the fluorescent decay of tryptophan residues in several proteins has been interpreted as involving motions in a cone of semiangle as large as $\sim 30°$ with relaxation times as short as 0.14 ns. Most of the published data on tryptophan residues is on the nanosecond time scale, so that the effect of faster motions can be detected only by the apparent reduction in the zero-time anisotropy (r_0). In particular, steady-state fluorescence anisotropy studies under conditions of oxygen quenching have resulted in a series of high-precision values for $(r_0)_{eff}$, the residual anisotropy at about 1 ns (Lakowicz & Weber, 1973a,b, 1980; Lakowicz et al., 1983).

From molecular dynamics simulations of proteins (Karplus & McCammon, 1981), it is clear that significant motion takes place on the picosecond time scale. Analysis has shown that the dominant contributions to the mean-square displacements come from fluctuations with a time scale of from 0.2 to ~ 10 ps in most cases (Karplus & McCammon, 1981; Swaminathan et al., 1982), and a detailed study of tyrosine ring oscillations in the pancreatic trypsin inhibitor has shown that the correlation function for the ring rotation angle, $\langle \Delta\phi(0)\Delta\phi(t) \rangle$, decays to zero in 0.2 ps (McCammon et al., 1979). However, for the fluorescence anisotropy of an aromatic ring such as tyrosine (PTI contains no tryptophans), it is not the correlation function for fluctuations of the ring angle but rather the second Legendre polynomial, P_2, of the cosine of the angle between the absorption and emission dipole vectors that is involved (Wallach, 1967). In an analysis of P_2 for the tyrosines in PTI based on a simulation in a van der Waals solvent (van Gunsteren & Karplus, 1982), it was found that for three out of four tyrosines the correlation function P_2 decays from its initial value of unity to a plateau value of ~ 0.8 in less than 2 ps and then remains essentially constant for the rest of the run; for the fourth tyrosine, which is on the surface of the molecule, the P_2 value continued to decay over the entire run. Consequently, the measured value of $(r_0)_{eff}$ on a nanosecond time scale should be significantly reduced relative to the ideal value ($r_0 = 0.4$) expected when the absorption and emission dipoles coincide. This important point was made in an analogous but more detailed analysis of the same tyrosines by Levy & Szabo (1982), based on a vacuum simulation of PTI provided by Karplus & McCammon (1979). They expressed the results in the form $(r_0)_{eff} = S^2 r_0$, where S^2 is a generalized order parameter (Levy et al., 1982; Lipari & Szabo, 1982), and found values of $(r_0)_{eff}$ similar to those calculated from the solvent run. Kasprzak & Weber (1982) have recently reported results of stationary state fluorescence polarization measurements of the tyrosines in PTI which are consistent with such a reduced value of $(r_0)_{eff}$; the average reduction estimated from the tyrosine data is 0.78, although as pointed out by the authors the interpretation in terms of tyrosine motion is not unequivocal. Since most experimental measurements of fluorescence depolarization have been made on tryptophans in a variety of proteins (Lakowicz & Weber, 1973a,b, 1980; Munro et al., 1979; Lakowicz et al., 1983), it appears worthwhile to extend the tyrosine analysis (van Gunsteren & Karplus, 1982; Levy & Szabo, 1982) to the fluorescence anisotropy of tryptophans. For this purpose, we have used a molecular dynamics simulation of hen egg white lysozyme calculated with the program CHARMM (Brooks et al., 1983). Lysozyme is a particularly convenient candidate for such a theoretical analysis because it contains six tryptophan residues in a variety of environments, so that their range of motional behavior should reflect that expected for most proteins.

The method used for the calculations is presented first, followed by the results and discussion; finally, the conclusions are summarized. An appendix is included to derive the form of the required correlation function for an anisotropic chromophore free to move in a rotating macromolecule.

Procedures

The molecular dynamics simulation method and the empirical potential function for proteins have been described previously (McCammon et al., 1979; Karplus & McCammon, 1981; Brooks et al., 1983); the details of the specific calculation will be given separately. The lysozyme molecule with 129 amino acids and 1001 heavy atoms is modeled by using extended atoms; i.e., hydrogens are not considered separately but are treated as part of the heavy atom to which they are attached (Gelin & Karplus, 1975, 1979; McCammon et al., 1977). After an equilibration period of 26 ps, the simulation was continued for an additional 34 ps, which served for the analysis; a time step of 0.001 ps was used, and the mean temperature of the run was 304 K. The required correlation functions and other dynamical information were obtained from a subset of 3400 coordinates spaced at intervals of 0.01 ps.

Corresponding molecular dynamics simulations have been made to study PTI in vacuum (McCammon et al., 1977, 1979; Karplus & McCammon, 1979; van Gunsteren & Karplus, 1982) and in a crystalline and solution environment (van Gunsteren & Karplus, 1982). The observed differences in the simulation results between those done in vacuum and in a solution or crystal environment are rather small, especially for interior atoms (van Gunsteren & Karplus, 1982). In particular, the magnitudes of fluctuations of atoms in the interior of proteins are essentially the same, although there appears to be a small increase in the relaxation times of the fluctuations in the solvent environment (Swaminathan et al., 1982). The simulation used for the lysozyme molecule was done in vacuum with no water molecules included. Since none of the tryptophans in lysozyme are completely exposed, the results for the simulation of lysozyme in vacuum should be relatively realistic and comparable to the behavior expected for lysozyme in solution.

For simplicity, the simulation used the same potential energy terms for the tryptophan when it is in the excited state as when it is in the ground state. Thus, any effect of the change in the

charge distribution of the excited state on the interaction potential is neglected, and the possibility of relaxation of the protein in the neighborhood of an excited chromophore is not included in the dynamics.

The fluorescence emission anisotropy, $r(t)$, at time t after excitation of the chromophore is generally defined by the expression (Wallach, 1967)

$$r(t) = \frac{I_{\parallel}(t) - I_{\perp}(t)}{I_{\parallel}(t) + 2I_{\perp}(t)} \tag{1}$$

where $I_{\parallel}(t)$ and $I_{\perp}(t)$ are the fluorescence intensities polarized parallel and perpendicular, respectively, to the polarization of the incident beam at time t. To evaluate the right-hand side of eq 1, we need explicit expressions for $I_{\parallel}(t)$ and $I_{\perp}(t)$. For this purpose, it is convenient to define a laboratory coordinate system L fixed in space so that the exciting light travels in the Y_L direction and is polarized along the Z_L axis (Wallach, 1967). The fluorescence is observed by using a perpendicular geometry; i.e., the observed light travels along the X_L axis, with $I_{\parallel}(t)$ corresponding to light polarized in the Z_L direction and $I_{\perp}(t)$ to light polarized in the Y_L direction. Let $\mu_A'(t)$ and $\hat{\mu}_E'(t)$ be unit vectors at time t directed along the chromophore absorption and emission dipole moments, respectively. A moving right-handed coordinate system A is defined with the z axis along $\hat{\mu}_A'(t)$, and a moving coordinate system E is defined with the z axis along $\hat{\mu}_E'(t)$; the y axes of the two systems are taken to be coincident, i.e., perpendicular to the plane defined by $\hat{\mu}_A'$ and $\hat{\mu}_E'$. The Euler angles $\Omega_{LA}(t) = [\alpha_{LA}(t), \beta_{LA}(t), \gamma_{LA}(t)]$ and $\Omega_{LE}(t) = [\alpha_{LE}(t), \beta_{LE}(t), \gamma_{LE}(t)]$ specify the transformation from the laboratory coordinate system L to the absorption and emission moment coordinate systems A and E, respectively. We are concerned with absorption at time $t = 0$ and emission at time t; thus, $\Omega_{LA}(0) = \Omega_{LA}$ is constant for a given chromophore while $\Omega_{LE}(t)$ varies with the time t. By simple geometric arguments, the probability that the molecule is excited at time $t = 0$ is proportional to

$$|\hat{\mu}_A'\cdot Z_L|^2 = \cos^2 \beta_{LA} \tag{2}$$

and the probabilities of emission at time t polarized along Z_L and Y_L are proportional to

$$|\hat{\mu}_E'(t)\cdot Z_L|^2 = \cos^2 \beta_{LE}(t) \tag{3a}$$

and

$$|\hat{\mu}_E'(t)\cdot Y_L|^2 = \sin^2 \beta_{LE}(t) \cos^2 \alpha_{LE}(t) \tag{3b}$$

respectively. The fluorescence intensity at time t is proportional to the probability that the chromophore is excited at $t = 0$ times the probability that it emits at time t; we have

$$I_{\parallel}(t) \propto \cos^2 \beta_{LA} \cos^2 \beta_{LE}(t) \tag{4a}$$

$$I_{\perp}(t) \propto \cos^2 \beta_{LA} \sin^2 \beta_{LE}(t) \cos^2 \alpha_{LE}(t) \tag{4b}$$

To apply eq 4a,b to a real system, we have to average the results over an ensemble of chromophores at equilibrium; for protein molecules in solution, this corresponds to an isotropic initial orientation of the chromophore. When the appropriate averaging is performed and the results are substituted into eq 1, the proportionality constants cancel, and a simple correlation function expression is obtained for $r(t)$ (Tao, 1969; Kinosita et al., 1977; see Appendix); we find

$$r(t) = \tfrac{2}{5}\langle P_2[\hat{\mu}_A'(0)\cdot\hat{\mu}_E'(t)]\rangle \tag{5}$$

Here $P_2(x)$ is the second-order Legendre polynomial, and the broken brackets denote an ensemble average.

When eq 5 is applied to a protein molecule, which is much larger than the fluorescent probe (a tryptophan residue of lysozyme in this case), the fast oscillations of the probe can be uncoupled from the much slower rotational motion of the protein. If the overall rotation is diffusional and isotropic, the anisotropy is given by (Wallach, 1967; Levy & Szabo, 1982; see Appendix)

$$r(t) = \tfrac{2}{5}e^{-t/\tau_m}\langle P_2[\hat{\mu}_A(0)\cdot\hat{\mu}_E(t)]\rangle \tag{6}$$

where τ_m is the correlation time for the overall rotation of the protein and $\hat{\mu}_A$ and $\hat{\mu}_E$ are the unit transition dipole vectors with components defined in a local coordinate system fixed in the molecule. For lysozyme, the overall tumbling can be described to a good approximation as isotropic (Dill & Allerhand, 1979), with a rotational correlation time at 300 K in aqueous solution of about 8 ± 2 ns (Gill et al., 1967; Dubin et al., 1971; Bauer et al., 1975; Dill & Allerhand, 1979). Thus, for the picosecond internal motions of the tryptophan side chain considered in this paper, the conditions for the validity of eq 6 are satisfied (Levy et al., 1981a,b; Lipari & Szabo, 1982).

The time development of the fluorescence anisotropy will be studied by means of eq 6 evaluated from the trajectory results. Since the simulation is done for a molecule in vacuum with no net translation or rotation, the quantity $\langle P_2[\hat{\mu}_A(0)\cdot\hat{\mu}_E(t)]\rangle$ is calculated directly, so that the internal motional contribution to the time dependence of $r(t)$ is obtained independent of the overall protein motion. The ensemble average of the correlation function at time t_m, $\langle P_2[\hat{\mu}_A(0)\cdot\hat{\mu}_E(t_m)]\rangle$, is estimated from a time average over the simulation by

$$\langle P_2[\hat{\mu}_A(0)\cdot\hat{\mu}_E(t_m)]\rangle \simeq (N-m)^{-1}\sum_{n=1}^{N-m} P_2[\hat{\mu}_A(t_n)\cdot\hat{\mu}_E(t_n + t_m)] \tag{7}$$

where the vectors $\hat{\mu}_A$ and $\hat{\mu}_E$ at times t_n and $t_n + t_m$, respectively, are calculated from the trajectory. If the fluorescence depolarization measurements were made on a molecule in a solid or rigid glass, the entire decay of $r(t)$ would come from this term. In solution, there is the additional time dependence of $r(t)$ due to overall rotation, which appears in the factor e^{-t/τ_m} of eq 6.

For a residue in a protein, the range of motions is generally restricted (McCammon et al., 1979) so that $\langle P_2[\hat{\mu}_A(0)\cdot\hat{\mu}_E(t)]\rangle$ is not expected to decay to zero. In fact, the correlation function will usually decay, possibly with oscillations, to a plateau on a picosecond time scale. If the internal motions decay exponentially with a relaxation time τ_1 and reach a plateau value P_∞, we have for the case that $\hat{\mu}_E(0)$ and $\hat{\mu}_A(0)$ are parallel (van Gunsteren & Karplus, 1982)

$$\langle P_2[\hat{\mu}_A(0)\cdot\hat{\mu}_E(t)]\rangle = (1 - P_\infty)e^{-t/\tau_1} + P_\infty \tag{8}$$

and from eq 6

$$r(t) = r_0[(1 - P_\infty)e^{-t/\tau_1} + P_\infty]e^{-t/\tau_m} \tag{9}$$

A slightly more complicated but realistic case corresponds to an internal correlation function which separates into two time scales ($\tau_1 \ll \tau_2 \ll \tau_m$), so we can write

$$\langle P_2[\hat{\mu}_A(0)\cdot\hat{\mu}_E(t)]\rangle = [(1 - P_\infty^1)e^{-t/\tau_1} + P_\infty^1][(1 - P_\infty^2)e^{-t/\tau_2} + P_\infty^2] \tag{10}$$

which yields

$$r(t) = r_0[(1 - P_\infty^1)e^{-t/\tau_1} + P_\infty^1][(1 - P_\infty^2)e^{-t/\tau_2} + P_\infty^2]e^{-t/\tau_m} \tag{11}$$

If the first term in brackets involves a correlation time τ_1 that

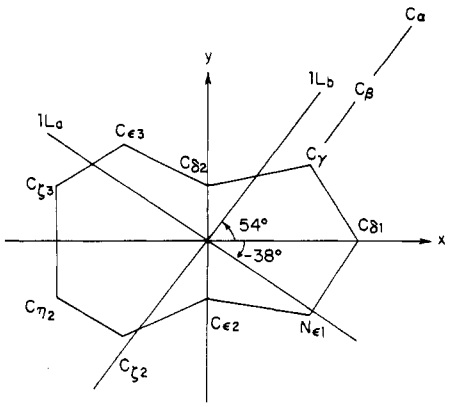

FIGURE 1: Directions of the transition moments of the ^1L_a and ^1L_b states of the tryptophan side chain determined experimentally from polarized absorption spectra of 3-indoleacetic acid and glycyl-L-tryptophan dihydrate (Yamamoto & Tanaka, 1972).

is short compared with present observational limits (i.e., in the picosecond range), we have

$$r(t) = (r_0)_{eff}[(1 - P_\infty^2)e^{t/\tau_2} + P_\infty^2]e^{-t/\tau_m} \quad (12)$$

where

$$(r_0)_{eff} = P_\infty{}^1 r_0 = S^2 \quad (13)$$

with S^2 ($0 \leq S^2 \leq 1$) the picosecond generalized order parameter (Levy et al., 1981a,b; Lipari & Szabo, 1982). This expression corresponds to that often used in the experimental analyses of spectra, where the quantity $r(t)$ is written in the form (Lakowicz et al., 1982)

$$r(t) = (r_0)_{eff}[\alpha e^{-t/\tau} + (1 - \alpha)]e^{-t/\tau_m} \quad (14)$$

with $\tau = \tau_2$ and $\alpha = 1 - P_\infty^2$ from eq 12.

The portion of the decay that is studied by the molecular dynamics simulation yields $(r_0)_{eff}$. The longer time decay due to internal motion corresponding to the relaxation time τ_2 is observable experimentally (e.g., 100 ps $\leq \tau_2 \leq$ 1 ns); examples are given in the work of Munro et al. (1979) and Lakowicz et al. (1983). As the separability of the time scales breaks down, only effective values for the relaxation times can be determined, as has been pointed out by Lipari & Szabo (1982) in their analysis of NMR parameters.

To employ eq 7 and the above formulation to evaluate the fluorescence anisotropy from the dynamics trajectory, it is necessary to know the orientations of $\hat{\mu}_A$ and $\hat{\mu}_E$ for the tryptophan chromophore itself. The excitation and emission spectra of tryptophan and other indole derivatives appear to involve two states, usually labeled ^1L_a and ^1L_b in analogy to the spectra of aromatic hydrocarbons (Konev, 1967; Song & Kurtin, 1969; Andrews & Forster, 1974), with transition moments in the plane of the rings at angles of −38° and 54°, respectively, to the long axis of the molecule (Yamamoto & Tanaka, 1972) (see Figure 1). The ^1L_a state has a much larger transition moment; irradiation at a wavelength of 300 nm (Lakowicz & Weber, 1973a,b, 1980; Munro et al., 1979; Lakowicz et al., 1983) leads almost exclusively to excitation of that state (Konev, 1967). Also, for this choice of wavelength, there is little intertryptophan transfer or excitation of tyrosines (Weber, 1960a,b). The exact nature of the emission is not fully characterized but appears to involve both the ^1L_a and ^1L_b states, the latter apparently due to vibronic coupling. Emission is usually observed at 340 (Munro et al., 1979) or 344 nm (Lakowicz & Weber, 1980; Lakowicz et al., 1983), where the contribution of ^1L_b is expected to be small but not necessarily zero (Valeur & Weber, 1977).

Before attempting to compare the calculated correlation functions with measurements of $(r_0)_{eff}$, it is necessary to consider the results of experiments which have attempted to determine the actual r_0 value for tryptophan. Measurements of *N*-acetyl-L-tryptophanamide and tryptophan-containing peptides and proteins in propylene glycol at −58 °C (Lakowicz et al., 1983) yielded r_0 values (denoted r_0') in the range 0.26–0.28, significantly lower than the theoretical limiting value of 0.4 for parallel absorption and emission dipoles (eq 6). The cause of the apparent reduction of the initial anisotropy is not known. Suggested explanations include mixing of ^1L_a and ^1L_b transitions in either absorption (Valeur & Weber, 1977) or emission (Song & Kurtin, 1969) and changes in the direction of the dipole moment of the ^1L_a excited state due to interaction with the solvent (Sun & Song, 1977), to exciplex formation (Walker et al., 1967), or to torsional vibrations (Jablonski, 1965). We treat some of these possibilities in the following section.

Results and Discussion

The correlation function $P_2(t) = \langle P_2[\hat{\mu}_A(0)\cdot\hat{\mu}_E(t)]\rangle$ was evaluated from the simulation for the six tryptophans of lysozyme by using several models in view of the uncertainty about the spectral properties of tryptophan. The simplest is the one where the tryptophan absorption and emission are due entirely to the unperturbed ^1L_a state, and therefore, the transition moment vectors $\hat{\mu}_A$ and $\hat{\mu}_E$ have identical directions in the molecule frame. To investigate the possibility that $\hat{\mu}_A$ and $\hat{\mu}_E$ have different orientations due to a perturbation of the ^1L_a excited state, we assume that $\hat{\mu}_A$ corresponds to the ^1L_a absorption and that $\hat{\mu}_E$ is in the plane of the tryptophan ring but makes an angle λ ($\lambda \cong \pm 30°$) with $\hat{\mu}_A$. Finally, we examine the result expected if the observed emission is a superposition of contributions from the two transitions $^1L_a \rightarrow {}^1A$ and $^1L_b \rightarrow {}^1A$, where ^1A represents the ground state and it is assumed that rapid thermalization of the ^1L_a and ^1L_b populations due to internal conversion has taken place prior to emission.

Ideal Case. For the case in which absorption and emission are due solely to the unperturbed ^1L_a transition, $\hat{\mu}_A$ and $\hat{\mu}_E$ are taken to be parallel and oriented at ∼−40° from the long axis, as indicated in Figure 1. Since the structure of the rings varies with time in the simulation, a transition moment direction was defined by using the vector that passes through $N_{\epsilon 1}$ and a point one-fifth of the distance along the bond between $C_{\epsilon 3}$ and $C_{\zeta 3}$ (see Figure 1); this vector is directed at −41° to the long axis. The results obtained for $P_2(t)$ for the different residues in this case show a wide range of behavior (Figure 2). For residues 108 and 123, $P_2(t)$ reaches a clear plateau value of 0.94 and 0.89, respectively, in less than 1 ps; for residues 63 and 111, $P_2(t)$ reaches a plateau value of 0.84 and 0.76 in about 6 ps, while for residues 28 and, particularly, 62, the values of $P_2(t)$ decay significantly out to 15 ps, the maximum time for which the correlation function results are meaningful. The correlation function $P_2(t)$ at t = 2 ps and the average of P_2 for the period $10 \leq t \leq 15$ ps for the six tryptophans are listed in Table I. It is evident from the calculated decay behavior that an extrapolation to "zero time" by the techniques presently in use for measuring tryptophan fluorescence (i.e., zero time is 0.5–1.5 ns; Munro et al., 1979; Lakowicz & Weber, 1973a,b, 1980; Lakowicz et al., 1983) would yield $(r_0)_{eff}$ values (eq 12 and 13) between 0.38 and 0.14 or even lower, relative to the ideal theoretical value of r_0 = 0.4 valid for $\hat{\mu}_A$ parallel to $\hat{\mu}_E$.

The above results can be used to estimate the contribution of the torsional vibrations of the tryptophan ring to the reduced value of r_0' obtained for *N*-acetyl-L-tryptophanamide in pro-

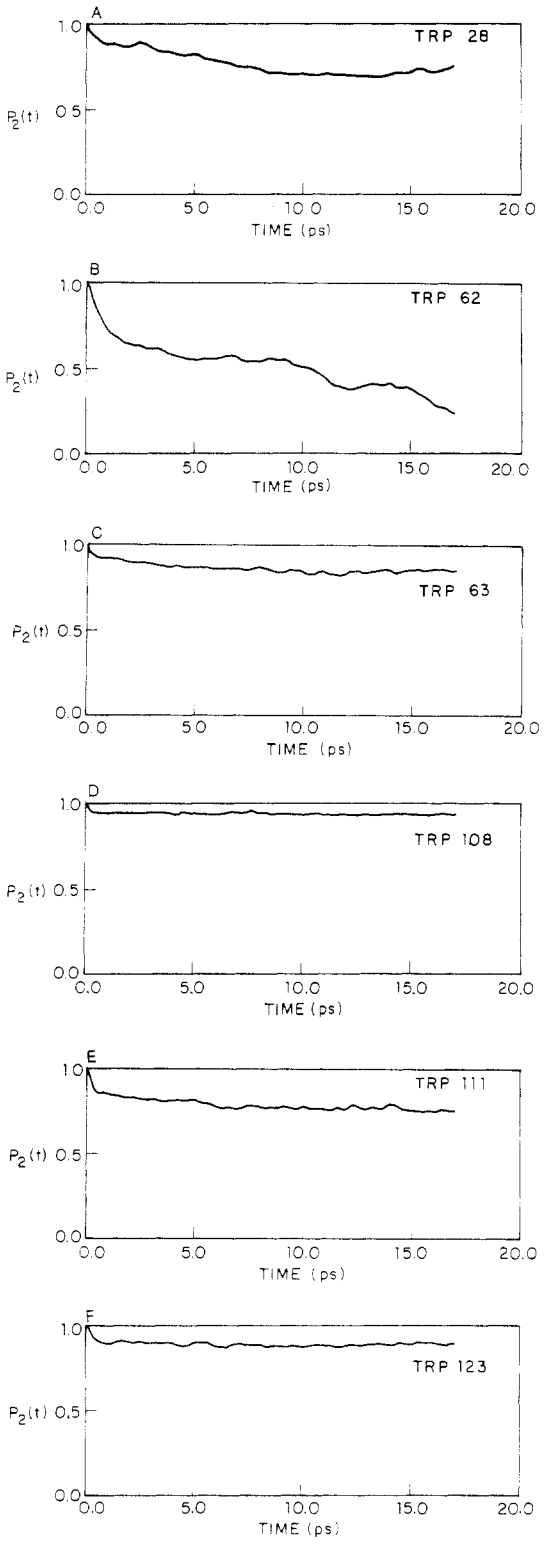

FIGURE 2: Correlation function $\langle P_2[\hat{\mu}(0)\cdot\hat{\mu}(t)]\rangle$ calculated from the simulation with $\hat{\mu}$ at −41° to the long axis: (A) Trp-28; (B) Trp-62; (C) Trp-63; (D) Trp-108; (E) Trp-111; (F) Trp-123.

pylene glycol at −58 °C (r_0' = 0.26–0.28). In the present simulation, the tryptophan with the least rotation, Trp-108, has an $(r_0)_{eff}$ of 0.38. Since it presumably has at least as much motion as a tryptophan in a rigid medium at low temperatures, torsional vibrations apparently are not the cause of the reduction of r_0' from the theoretical value of 0.4.

Perturbed Electronic State. If the value of r_0' in *N*-acetyl-L-tryptophanamide is due solely to a difference in the orientation of the chromophore absorption and emission dipoles, the magnitude of the angle λ between the two vectors can be estimated from

$$\frac{r_0'}{0.4} \cong P_2(\cos\lambda) = \frac{3\cos^2\lambda - 1}{2} \qquad (15)$$

Using Lakowicz's value of r_0' = 0.26, we find $\lambda \approx \pm 30°$. To investigate the effect of such a deviation in angle, we calculated the correlation function (eq 7) by assuming that the absorption is at −41° (^1L_a state) and that the emission vector is at −10° or −70° to the long axis; this choice, made for ease of calcu-

Table I: Tryptophan Fluorescence Depolarization

residue	(A) Ideal emission at −41° P_2 (t = 2 ps)	P_2 (15 ps ⩾ t ⩾ 10 ps)
28	0.88	0.71
62	0.64	0.36
63	0.89	0.84
108	0.94	0.94
111	0.84	0.76
123	0.90	0.89

residue	(B) Perturbed Excited State emission at −10° $P_2^{+30°}$ (t = 2 ps)	$P_2^{+30°}$ (15 ⩾ t ⩾ 10 ps)	emission at −70° $P_2^{-30°}$ (t = 2 ps)	$P_2^{-30°}$ (15 ⩾ t ⩾ 10 ps)
28	0.54	0.41	0.54	0.42
62	0.49	0.57	0.33	−0.05
63	0.53	0.46	0.57	0.57
108	0.56	0.54	0.61	0.62
111	0.48	0.46	0.53	0.45
123	0.54	0.62	0.58	0.49

residue	(C) Internal Conversion emission at −41° and 55° P_2 (t = 2 ps)	P_2 (15 ⩾ t ⩾ 10 ps)
28	0.56	0.44
62	0.42	0.25
63	0.58	0.54
108	0.61	0.61
111	0.53	0.48
123	0.59	0.57

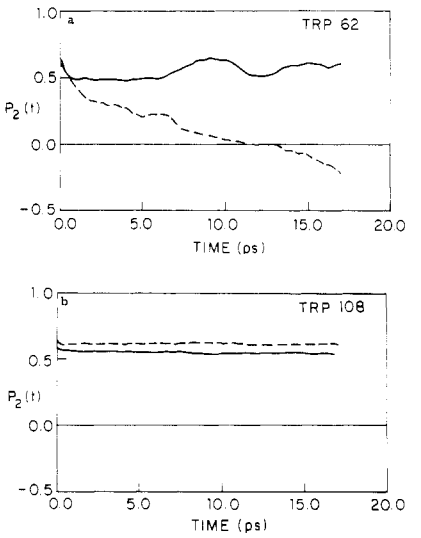

FIGURE 3: Correlation function $\langle P_2[\hat{\mu}_A(0)\cdot\hat{\mu}_E(t)]\rangle$ calculated from the simulation with $\hat{\mu}_A(0)$ at −41° to the long axis and $\hat{\mu}_E(0)$ at −10° (solid line) or −70° (dashed line): (a) Trp-62; (b) Trp-108. The value at time zero is $P_2(\cos 31°)$ for $\hat{\mu}_E(0)$ at −10° and $P_2(\cos 29°)$ for $\hat{\mu}_E(0)$ at −70° (see text).

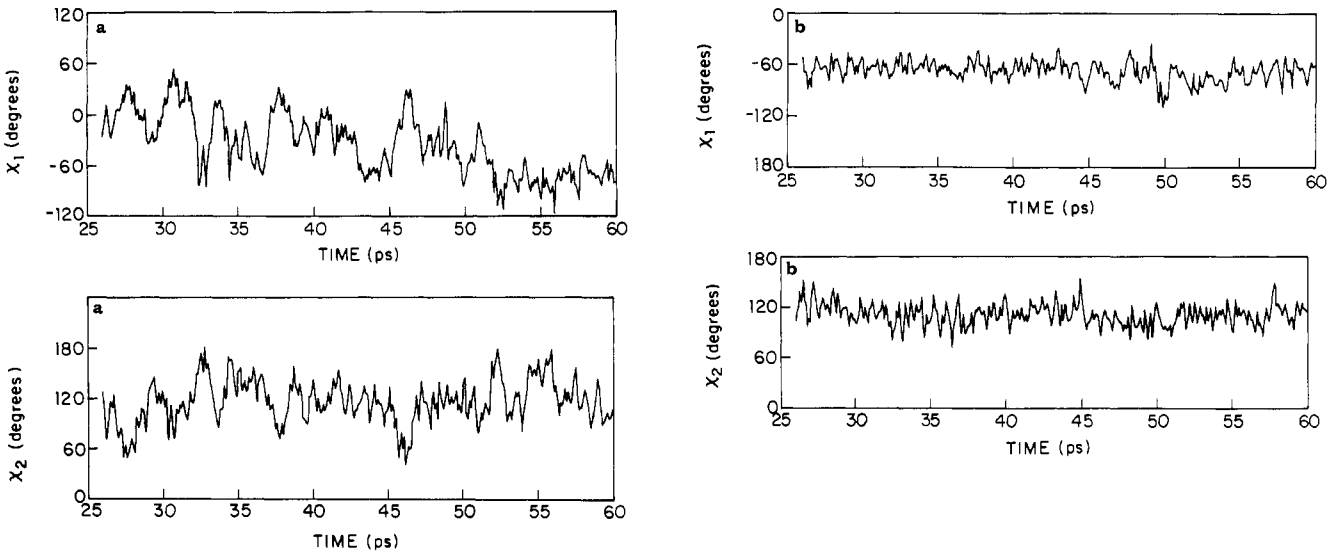

FIGURE 4: Time series for χ_1 and χ_2: (a) Trp-62; (b) Trp-123.

lation, corresponds to $\lambda = +31°$ and $\lambda = -29°$, respectively. The resulting correlation functions, $P_2^+(t)$ and $P_2^-(t)$, have initial values equal to $P_2(\cos\lambda)$ and, except for Trp-62, decay in a manner similar to that of $P_2(t)$ for $\hat{\mu}_A$ and $\hat{\mu}_E$ parallel. Figure 3 shows the results for Trp-62 and a more typical residue, Trp-108; the values for $P_2^+(0)$ and $P_2^-(0)$ are not exactly equal because the angles between the absorption and emission vectors are slightly different.

If certain symmetry conditions are satisfied (see Appendix), the anisotropy given by eq 6 reduces to

$$r(t) = \tfrac{2}{5}e^{-t/\tau_m}P_2(\cos\lambda)\langle P_2[\hat{\mu}(0)\cdot\hat{\mu}(t)]\rangle \qquad (16)$$

where $\hat{\mu}(t)$ is either $\hat{\mu}_A$ or $\hat{\mu}_E$. Thus, the ratios $P_2^+(t)/P_2(\cos\lambda)$ and $P_2^-(t)/P_2(\cos\lambda)$ become equal to $P_2(t)$ calculated for $\hat{\mu}_A$ and $\hat{\mu}_E$ parallel. From Table I, we see that for all tryptophan residues, except for Trp-62, the above relation is true to within ~15%. Although the symmetry conditions for the validity of eq 16 are not satisfied by tryptophans in a protein (see Appendix), it is likely that the large deviations observed for Trp-62 are due to slow motions that are not fully averaged. In the trajectory, Trp-62 is undergoing a slow rotation about the C_α–C_β axis which is approximately perpendicular to the ring (see Figure 4); the rotation corresponds to a clockwise motion in Figure 1. Thus, for Trp-62, if $\hat{\mu}_E$ is at −10° to the long axis, it tends to rotate toward the initial position of $\hat{\mu}_A$, and if $\hat{\mu}_E$ is at −70°, it tends to rotate away from it.

For certain cases (e.g., Trp-62 emission at −10°; see Table I), the anisotropy increases above the initial value. This is a nonequilibrium effect due to the limited time of the trajectory in which there is a net rotation of the emission vector toward the initial position of the absorption vector so that the angle defined by $\hat{\mu}_A(0)\cdot\hat{\mu}_E(t)$ is less than λ. In a true equilibrium, $r(t)$ will always be less than or equal to $r(0)$.

The range of $(r_0)_{eff}$ values for the present case is 0.16 to 0.25 for $\hat{\mu}_E$ at −10° to the long axis ($\lambda \cong +30°$) and −0.02 to 0.25 for $\hat{\mu}_E$ at −70° to the long axis ($\lambda \cong -30°$).

Internal Conversion. Another possible cause for the observed value of r_0' in *N*-acetyl-L-tryptophanamide is partial internal conversion from the ^1L_a to the ^1L_b state before emission. We assume that the internal conversion rate is fast relative to the fluorescence and that the ^1L_a and ^1L_b populations are in equilibrium so that the fraction of emission from each state is a constant (Andrews & Forster, 1974; Robbins et al., 1980). Since internal conversion for typical organic molecules occurs with a lifetime of 0.01–10 ps (Cowan & Drisko, 1976), the assumption is reasonable on the experimental nanosecond time scale [i.e., for the evaluation of $(r_0)_{eff}$]. However, the short-time anisotropy calculated from the simulation would be affected by any time dependence of the emission ratio in the picosecond range. If $r_a(t)$ and $r_b(t)$ are the anisotropies for emission from the ^1L_a and ^1L_b states, respectively, we can write the total emission anisotropy in the form (Valeur & Weber, 1977)

$$r(t) \cong (1-f)r_a(t) + fr_b(t) \qquad (17)$$

where f is the fraction of emission due to the ^1L_b state. Assuming that the directions of the ^1L_a and ^1L_b transition moments are the same for emission and absorption, we have $r_a(0) = 0.4$ and $r_b(0) = 0.4P_2(\cos\lambda')$ where λ' is the angle between the ^1L_a and ^1L_b transition moment vectors. Since the ^1L_b moment is at approximately 55° to the long axis (the vector passes through a point three-tenths of the distance between $C_{\zeta 2}$ and $C_{\epsilon 2}$ and a point halfway between $C_{\delta 2}$ and C_γ; see Figure 1), the angle $\lambda' = 84°$, and consequently $r_b(0) = -0.19$. With the measured value $r_0' = 0.26$, we find $f = 0.17$.

The correlation functions of the various residues for emission from the ^1L_b state are shown as dashed lines in Figure 5). They all start at the initial value of −0.48, close to the minimum possible value ($P_2 = -0.5$), corresponding to an angle of 90°, and increase to a plateau, except for Trp-62 which is still increasing after 16 ps. The total anisotropy obtained from eq 17 with $f = 0.17$ is shown as the solid line in Figure 5. The inclusion of emission from ^1L_b does not affect the percent decay significantly; that is, $(r_0)_{eff}/[r(0)]$ for dual emission is approximately equal to $(r_0)_{eff}/[r(0)]$ for emission solely from the ^1L_a state (see Table I).

The range of values of $(r_0)_{eff}$ calculated for the different tryptophans under the present assumption is 0.10–0.24. The value of $(r_0)_{eff}$ calculated from this model is very close to the average of the values for $\lambda = +30°$ and −30° calculated from the perturbed electronic-state model (see above) because of the near-90° orientation of the ^1L_a and ^1L_b transition moments; if the two are exactly perpendicular, the internal conversion result is the same as this average.

Comparison with Experiment. The studies of tryptophan fluorescence anisotropy on the subnanosecond time scale by Munro et al. (1979), for proteins containing single tryptophans, have yielded extrapolated $(r_0)_{eff}$ values between 0.18 and 0.26. Lakowicz & Weber (1980) have measured lifetime-resolved fluorescence anisotropies in a series of proteins with a minimum quenching time of 1.6 ns. Their results for $(r_0)_{eff}$ cluster

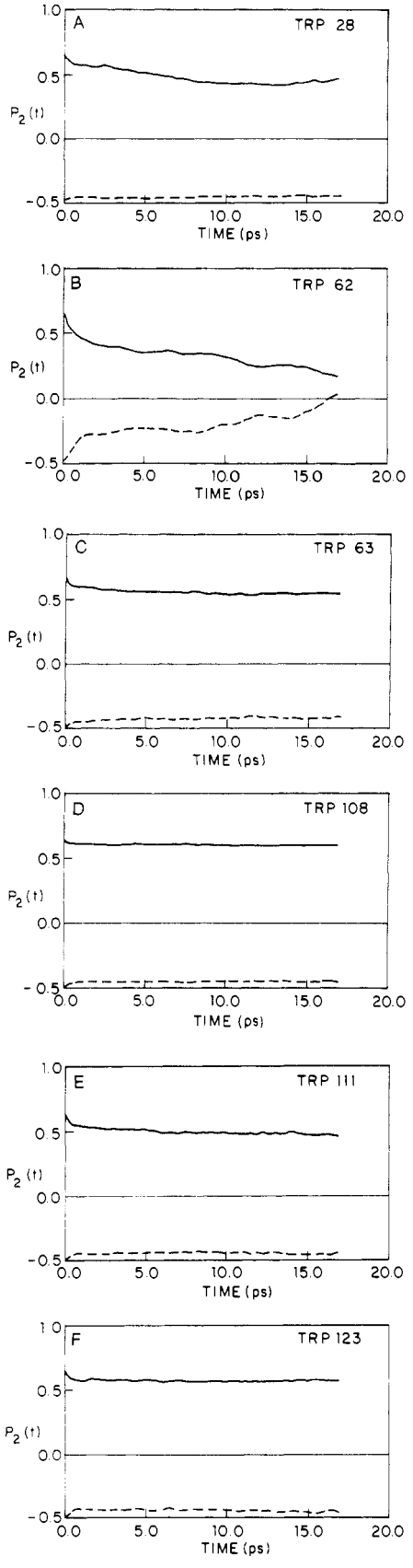

FIGURE 5: Correlation function $\langle P_2[\hat{\mu}_A(0)\cdot\hat{\mu}_E(t)]\rangle$ calculated from the simulation with $\hat{\mu}_A(0)$ at −41° and $\hat{\mu}_E(0)$ at +54° to the long axis (dashed line) and the combined function for $\hat{\mu}_A$ at −41° and $\hat{\mu}_E$ at −41° and +54° (see text): (A) Trp-28; (B) Trp-62; (C) Trp-63; (D) Trp-108; (E) Trp-111; (F) Trp-123.

between 0.24 and 0.30, except for carbonic anhydrase, which yields the significantly smaller value of 0.18. A more recent study by Lakowicz et al. (1983), in which they examined a series of proteins with one or more tryptophans, yielded values of $(r_0)_{eff}$ between 0.11 and 0.26. These results for a variety of proteins are consistent with the simulation values with the assumption that r_0' is reduced from the ideal value of 0.4 by a mechanism independent of tryptophan dynamics, that is, by one of the models involving the intrinsic vibronic behavior of a tryptophan chromophore (e.g., perturbed electronic state or internal conversion model).

Table II: Equal-Time Correlation for χ_1 and χ_2

residue	$\langle(\Delta\chi_1)^2\rangle^{1/2}$ (deg)	$\langle(\Delta\chi_2)^2\rangle^{1/2}$ (deg)	$\frac{\langle\Delta\chi_1\Delta\chi_2\rangle}{\langle(\Delta\chi_1)^2\rangle^{1/2}\langle(\Delta\chi_2)^2\rangle^{1/2}}$
28	10.2	19.4	−0.20
62	35.5	26.4	−0.61
63	11.9	15.3	−0.27
108	12.3	15.2	−0.78
111	10.5	21.9	−0.46
123	11.5	12.9	−0.24

For lysozyme itself, the presence of six tryptophans makes it difficult to analyze the available experimental data. However, a variety of studies suggest that about 80% of the fluorescence is due to two residues, Trp-62 and Trp-108 (Imoto et al., 1972a,b), both found in the active site (Blake et al., 1967) and that the fluorescence of the other tryptophan residues is quenched. Although oxidation of either Trp-62 or Trp-108 appears to reduce the fluorescence by close to 50%, it is not clear what the ratio of contributions is in the unoxidized system (Imoto et al., 1972a,b). Lifetime-resolved fluorescence anisotropy experiments for lysozyme (Lakowicz et al., 1982) at 25 °C indicate that the apparent correlation times are shorter than would be expected from overall protein tumbling, which has been interpreted as evidence for the presence of internal motions on a nanosecond time scale. The initial anisotropy, $(r_0)_{eff}$, is equal to 0.23, a value in the range of that observed for other proteins. If the value of $r_0' = 0.26$ is a consequence of the fact that $\hat{\mu}_E$ has a different orientation from $\hat{\mu}_A$ (see Perturbed Electronic State), the possible orientations of $\hat{\mu}_E$ relative to $\hat{\mu}_A$ are −10° and −70°. For −10°, the calculated $(r_0)_{eff}$ values for Trp-62 and -108 are 0.23 and 0.22, respectively, while for −70°, $(r_0)_{eff}$ is found to be −0.02 and 0.25, respectively. If Trp-62 and -108 do make approximately equal contributions to the observed fluorescence, $\hat{\mu}_E = -10°$ is in much better agreement with the observations. With the internal conversion model, the $(r_0)_{eff}$ values for Trp-62 and -108 are 0.10 and 0.24, respectively.

Nature of the Tryptophan Motions. Reorientation of the transition dipole vector of tryptophan is due mainly to rotation about the C_α–C_β and C_β–C_γ bonds, which correspond to the χ_1 and χ_2 dihedral angles of the side chain. In the protein environment, the fluctuations of χ_1 and χ_2 are expected to be anticorrelated so that large variations in the two angles result in smaller net motion of the bulky ring system. Figure 4 shows χ_1 and χ_2 as a function of time for Trp-62 and -123. We can estimate the degree of correlation by the equal-time cross-correlation function

$$C(\chi_1, \chi_2) = \frac{\langle\Delta\chi_1\Delta\chi_2\rangle}{\langle(\Delta\chi_1)^2\rangle^{1/2}\langle(\Delta\chi_2)^2\rangle^{1/2}}$$

where $\Delta\chi_j$ is the deviation of angle χ_j from its mean value. The results for the tryptophans of lysozyme are shown in Table II. It is evident that for large-angle fluctuations and small anticorrelation values, the P_2 motional averaging is greatest (see Table I). For example, comparing Trp-28 and -108, we see that the angular fluctuations are similar but that for

Table III: Root Mean Square Fluctuations (Å) for Tryptophans Estimated from Temperature Factors and Dynamics[a]

Trp residue	tetragonal HEWL[b]	triclinic HEWL[c]	human lysozyme[b]	dynamics[d]
28	0.693	0.440	0.640	0.605
62	1.430	0.705	1.456[e]	2.025
63	0.822	0.442	0.789	0.737
108	0.861	0.576	0.844	0.677
111	0.686	0.608	0.850	1.075
123	0.830	0.638	0.960[e]	0.662

[a] Average of rms values over all the ring atoms. [b] Results provided by D. C. Phillips (private communication); see Sternberg et al. (1979) and Blake et al. (1965). [c] Results provided by L. H. Jensen (private communication); see Kurachi et al. (1976). [d] Results from the 30-ps dynamic simulation for HEWL. [e] In human lysozyme, tyrosines are substituted for these tryptophans.

Trp-28, with the larger decay in P_2, the anticorrelation value is much less than that of Trp-108. For Trp-62 with the greatest decay, the anticorrelation is rather high, but the individual angular fluctuations are considerably larger than those for the other tryptophans. These results make clear that a model which treated each of the dihedral angles independently would not be valid in this case and, more generally, for side-chain motions in the interior of a protein (van Gunsteren & Karplus, 1982). This contrasts with the behavior of simple alkanes and exposed protein side chains where an uncorrelated model gives satisfactory results for dipolar relaxation of ^{13}C nuclei in NMR (Levy et al., 1981b).

To check that the decay of $P_2(t)$ arose primarily from reorientation of the ring as a whole rather than from internal motions (e.g., puckering of the ring), we used different vectors to calculate $P_2(t)$. The correlations for a "short" vector defined between atom $N_{\epsilon 1}$ and the point halfway between $C_{\delta 2}$ and $C_{\epsilon 2}$ were calculated and shown to be identical with the longer vector used in Table I. Also, the out of plane bending angles $C_{\delta 2}$–$C_{\epsilon 2}$–$C_{\epsilon 3}$–C_γ and $C_{\epsilon 2}$–$C_{\delta 2}$–$C_{\beta 2}$–$N_{\epsilon 1}$ were examined. The root mean square (rms) fluctuations of these angles are about 6–7°, and equal-time cross-correlations of the two angles indicate that they are highly anticorrelated (the angles are defined such that this means $C_{\delta 2}$ and $C_{\epsilon 2}$ move symmetrically perpendicular to the plane of the ring), so that these fluctuations make only a very small contribution to the decay of $P_2(t)$.

Comparisons with Other Results. It is of interest to compare the decay of $P_2(t)$ as calculated from the dynamics with other measures of side-chain motion; we consider here only the $P_2(t)$ results for $\hat{\mu}_A$ and $\hat{\mu}_E$ parallel; corresponding conclusions would apply to the calculations with $\hat{\mu}_A$ not parallel to $\hat{\mu}_E$. Table III lists the average root mean square (rms) fluctuations of tryptophans obtained from the temperature factors of two X-ray studies of hen egg white lysozyme (HEWL) and one from human lysozyme, as well as the rms values obtained from the dynamic simulation of HEWL. The calculated values of P_2 (t = 2 ps) in Table I are only roughly correlated with the rms fluctuations from the X-ray data and the dynamic simulation. It is clear that Trp-62 has the largest rms values in all cases and the greatest decay in $P_2(t)$. It is of interest in this regard that Trp-62 undergoes a large displacement (0.75 Å) on substrate binding (Blake et al., 1967). For the other tryptophans, the differences in the rms fluctuations are smaller and vary significantly from one molecule to another. There does not appear to be a direct correlation with the calculated behavior of $P_2(t)$.

Examination of the different local environment of the tryptophans shows some correlation with the P_2 values. In Table IV, we list the number of nearest neighbors, the percent accessibility relative to a free tryptophan, calculated according to the Lee and Richards criterion (Richards, 1977) for the average dynamical structure, and the hydrogen-bonded state of $N_{\epsilon 1}$ (Imoto et al., 1972b). Trp-108, which has the largest plateau value of $P_2(t)$, is inaccessible, has a large number (22) of close contacts, and is hydrogen bonded from $N_{\epsilon 1}$ to the carbonyl oxygen of residue 56. By contrast, Trp-62, the most mobile residue in terms of P_2, is accessible to the surface, has only eight close contacts, and is not hydrogen bonded.

Table IV: Environment of Tryptophans[a]

residue	no. of contacts <3.5 Å: backbone	no. of contacts <3.5 Å: side chain	hydrogen-bonded state of $N_{\epsilon 1}$[a]	accessibility[b] (%)
28	14	14	no	0
62	14	8	no	49
63	19	10	no	7
108	19	22	yes	0
111	15	5	yes	25
123	16	11	no	15

[a] According to Imoto et al. (1972b). [b] Percent accessibility relative to a free tryptophan.

Conclusions

It is evident from the fluorescence depolarization rates calculated for tryptophan residues in lysozyme that there is an important motional contribution on the picosecond time scale for some tryptophans and not for others. In spite of the larger size of the tryptophan side chain relative to tyrosine, the plateau of P_2 values found for some of the tryptophans in this simulation of lysozyme is of the same order as the ones calculated in PTI for the tyrosines (van Gunsteren & Karplus, 1982; Levy & Szabo, 1982). The wide variation in the behavior of the correlation functions and the resulting fluorescence depolarization rate calculated for the different tryptophans suggests that measurements with short-time resolution (e.g., employing femtosecond laser techniques) for systems with a single tryptophan (e.g., azurin) would be of great interest.

Appendix

Many previous derivations of the correlation functions for the motion of a probe in a macromolecule assume both cylindrical symmetry of the probe and azimuthal symmetry of its motion (Lipari & Szabo, 1980; Brainard & Szabo, 1981). These assumptions are not valid for the asymmetric tryptophan side chain in a restricted protein environment; the second also would not necessarily be correct for a tyrosine ring in the interior of a protein. The correlation function for an asymmetric probe which absorbs and emits in different directions and moves in an asymmetric potential is described here. The notation follows that of Brainard & Szabo (1981) as closely as possible.

We consider the fluorescence depolarization of a molecule in solution. Following a similar derivation by Wallach (1967, eq 37 and 43), the trigonometric functions in eq 4 can be related to elements of the Wigner rotation matrix, $D_{ab}^{(2)}$ (Brink & Satchler, 1971), and the resulting expressions substituted into eq 1 for $r(t)$ to give the emission anisotropy for a general anisotropic chromophore in the form

$$r(t) = 2\langle D_{00}^{(2)*}[\Omega_{LA}(0)] D_{00}^{(2)}[\Omega_{LE}(t)]\rangle \qquad \text{(A1)}$$

This basic result can be used to prove the necessary equations (eq 5, 6, and 16 of the text).

To prove eq 5, we make use of the fact that for an isotropic system (e.g., a molecule rotating freely in solution) $r(t)$ is

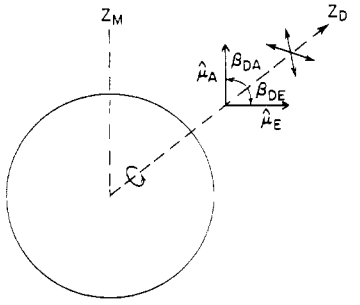

FIGURE 6: Schematic representation of a side chain within a protein, after Brainard & Szabo (1981). The absorption and emission dipoles, which are in the plane of the molecule, are not parallel to each other or to the Z_D axis.

independent of the direction of the z axis. This means we can average the right-hand side of eq A1 over $\hat{z}$ [i.e., $1/(4\pi)\int d\hat{z} = 1/(4\pi)\int_0^{2\pi} d\alpha \int_{-1}^{1} d\cos\beta$] to obtain

$$r(t) = \frac{2}{4\pi}\int \langle D_{00}^{(2)*}[\Omega_{LA}(0)] D_{00}^{(2)}[\Omega_{LE}(t)]\rangle \, d\hat{z} \quad (A2)$$

or

$$r(t) = \frac{2}{4\pi}\left\langle \int P_2[\cos\beta_{LA}(0)]\; P_2[\cos\beta_{LE}(t)]\; d\hat{z}\right\rangle \quad (A3)$$

where we have introduced the explicit expression for $D_{00}^{(2)}$ (Brink & Satchler, 1971); for simplicity, we omit the time dependence of the variables in what follows. Using the addition theorem for spherical harmonics

$$P_2(\cos\beta_{LE}) = \sum_{m=-2}^{2} C_{2m}(\beta_{LA}, \alpha_{LA}) C_{2m}^{*}(\beta_{AE}, \alpha_{AE}) \quad (A4)$$

and introducing associated Legendre polynomials for the modified spherical harmonics in eq A4, we find by substituting into eq A3

$$\begin{aligned} r(t) = \frac{2}{4\pi}\Bigg\langle \int d\hat{z}\; P_2(\cos\beta_{LA}) \times \\ \left\{\sum_m \frac{(2-m)!}{(2+m)!} P_2^m(\cos\beta_{LA})\; P_2^m(\cos\beta_{AE})\; e^{im(\alpha_{LA}-\alpha_{AE})}\right\}\Bigg\rangle = \\ \frac{1}{2\pi}\Bigg\langle \int_0^{\pi}\int_0^{2\pi} P_2(\cos\beta_{LA})\Big\{P_2^0(\cos\beta_{LA})\; P_2^0(\cos\beta_{AE}) + \\ \frac{2}{3!}P_2^1(\cos\beta_{LA})\; P_2^1(\cos\beta_{AE})\cos(\alpha_{LA}-\alpha_{AE}) + \\ \frac{2}{4!}P_2^2(\cos\beta_{LA})\; P_2^2(\cos\beta_{AE})\cos 2(\alpha_{LA}-\alpha_{AE})\Big\} \times \\ d\alpha_{LA}\sin\beta_{LA}\, d\beta_{LA}\Bigg\rangle \end{aligned} \quad (A5)$$

Integration over α_{LA} gives zero for the second and third terms in eq A5 and we obtain

$$\begin{aligned} r(t) = +\frac{1}{4}\int_0^{\pi} (9\cos^4\beta_{LA} - 6\cos^2\beta_{LA} + 1) \\ \sin\beta_{LA}\, d\beta_{LA}\langle P_2(\cos\beta_{AE})\rangle = -\frac{1}{4}\Bigg[9\frac{\cos^5\beta}{5}\Big|_0^{\pi} - \\ 6\frac{\cos^3\beta}{3}\Big|_0^{\pi} + \cos\beta\Big|_0^{\pi}\Bigg]\langle P_2[\hat{\mu}_A'(0)\cdot\hat{\mu}_E'(t)]\rangle \end{aligned} \quad (A6)$$

which yields

$$r(t) = \tfrac{2}{5}\langle P_2[\hat{\mu}_A'(0)\cdot\hat{\mu}_E'(t)]\rangle \quad (A7)$$

the general expression for $r(t)$ given in eq 5; in eq A6 and A7, we have reintroduced the time dependence of the variables.

To derive eq 6, we introduce an arbitrary coordinate system M, rigidly attached to the macromolecule (see Figure 6). The transformation from L to A or E may be written as a product of successive transformations from L to M and M to A or E (j = A or E):

$$D_{mn}^{(2)}[\Omega_{Lj}] = \sum_{a=-2}^{2} D_{ma}^{(2)}[\Omega_{LM}] D_{an}^{(2)}[\Omega_{Mj}] \quad (A8)$$

Substituting eq A8 into eq A1 and assuming that the internal motion of the probe and the overall motion of the macromolecule are uncoupled, we obtain

$$\begin{aligned} r(t) = 2\sum_{aa'}\langle D_{0a}^{(2)*}[\Omega_{LM}(0)] D_{0a'}^{(2)}[\Omega_{LM}(t)]\rangle \times \\ \langle D_{a0}^{(2)*}[\Omega_{MA}(0)] D_{a'0}^{(2)}[\Omega_{ME}(t)]\rangle \end{aligned} \quad (A9)$$

For isotropic motion of the macromolecule [see Appendix in Wallach (1967); Levy et al., 1981b]

$$\langle D_{0a}^{(2)*}[\Omega_{LM}(0)] D_{0a'}^{(2)}[\Omega_{LM}(t)]\rangle = \frac{\delta_{aa'}}{5} e^{-t/\tau_m} \quad (A10)$$

Using this expression in eq A9, we have

$$\begin{aligned} r(t) = \frac{2}{5}e^{-t/\tau_m}\sum_{a=-2}^{2}\langle D_{a0}^{(2)*}[\Omega_{MA}(0)] D_{a0}^{(2)}[\Omega_{ME}(t)]\rangle = \\ \frac{2}{5}e^{-t/\tau_m}\sum_{a=-2}^{2}\langle C_{2a}[\beta_{MA}(0), \alpha_{MA}(0)] C_{2a}^{*}[\beta_{ME}(t), \alpha_{ME}(t)]\rangle \end{aligned} \quad (A11)$$

where $C_{2a}(\beta, \alpha)$ are the modified spherical harmonics. By the addition theorem for spherical harmonics, eq A11 reduces to

$$r(t) = \tfrac{2}{5}e^{-t/\tau_m}\langle P_2[\hat{\mu}_A(0)\cdot\hat{\mu}_E(t)]\rangle \quad (A12)$$

which is the result given in eq 6.

Equations A7 and A12 were derived without any assumptions concerning the symmetry of the probe; eq A12 can be simplified when certain conditions apply. We define another coordinate system D with the y axis coincident with Y_A and Y_E and the z axis in the plane of Z_A and Z_E but not yet specified. The transformations from D to A and from D to E are determined by the Euler angles (0, β_{DA}, 0) and (0, β_{DE}, 0), respectively. Use of the transformation properties of eq A8 to introduce the coordinate system D into eq A11 yields

$$\begin{aligned} r(t) = \tfrac{2}{5}e^{-t/\tau_m}\sum_{abb'}\langle D_{ab}^{(2)*}[\Omega_{MD}(0)] D_{ab'}^{(2)}[\Omega_{MD}(t)]\rangle \times \\ d_{b0}^{(2)*}(\beta_{DA}) d_{b'0}^{(2)}(\beta_{DE}) \end{aligned} \quad (A13)$$

where $d_{ab}^{(2)}(\beta)$ are reduced Wigner rotation matrix elements (Brink & Satchler, 1971). If the dipole vectors $\hat{\mu}_A$ and $\hat{\mu}_E$ rotate freely with fixed polar angles about a unique symmetry axis C_∞ and if C_∞ is in the plane Z_A and Z_E, the coordinate system D can be defined such that Z_D lies along the C_β–C_γ bond (C_∞), which is in fact a poor assumption, and that the ring is coplanar with the C_β–C_γ bond, which is a good approximation. Furthermore, if Z_D moves in an azimuthally symmetric way about Z_M (see Figure 6), then the correlation function in eq A13 is nonzero only if $b = b'$, so that

$$\begin{aligned} r(t) = \tfrac{2}{5}e^{-t/\tau_m}\sum_{ab}\langle D_{ab}^{(2)*}[\Omega_{MD}(0)] D_{ab}^{(2)}[\Omega_{MD}(t)]\rangle \times \\ d_{b0}^{(2)}(\beta_{DA}) d_{b0}^{(2)}(\beta_{DE}) \end{aligned} \quad (A14)$$

Brainard & Szabo (1981) derived the corresponding equation for the case where $\hat{\mu}_A$ and $\hat{\mu}_E$ are parallel. Finally, if either $\hat{\mu}_A$ or $\hat{\mu}_E$ is parallel to Z_D (for example, $\hat{\mu}_A$ parallel to Z_D), then

$$r(t) = \tfrac{2}{5}e^{-t/\tau_m}\sum_{a}\langle D_{a0}^{(2)*}[\Omega_{MA}(0)] D_{a0}^{(2)}[\Omega_{MA}(t)]\rangle d_{00}^{(2)}(\lambda_{AE})$$

where λ_{AE} is the angle between $\hat{\mu}_A$ and $\hat{\mu}_E$. In terms of Legendre polynomials, $r(t)$ is

$$r(t) = \tfrac{2}{5}e^{-t/\tau_m}P_2(\cos\lambda_{AE})\langle P_2[\hat{\mu}_A(0)\cdot\hat{\mu}_A(t)]\rangle \quad \text{(A15)}$$

the expression given in eq 16. Lipari & Szabo (1980) derived a similar equation, although they did not explicitly state the result for the case of a rapidly fluctuating probe in a macromolecule.

Registry No. L-Tryptophan, 73-22-3; lysozyme, 9001-63-2.

References

Andrews, L. J., & Forster, L. S. (1974) *Photochem. Photobiol. 19*, 353.

Bauer, D. R., Opella, S. J., Nelson, D. J., & Pecora, R. (1975) *J. Am. Chem. Soc. 97*, 2580.

Blake, C. C. F., Koenig, D. F., Mair, G. A., North, A. C. T., Phillips, D. C., & Sarma, V. R. (1965) *Nature (London) 206*, 757.

Blake, C. C. F., Johnson, L. N., Mair, G. A., North, A. C. T., Phillips, D. C., & Sarma, V. R. (1967) *Proc. R. Soc. London, Ser. B 167*, 378.

Brainard, J. R., & Szabo, A. (1981) *Biochemistry 20*, 4618.

Brink, D. M., & Satchler, G. R. (1971) *Angular Momentum*, 2nd ed., Oxford University Press, Oxford.

Brooks, B. R., Bruccoleri, R. E., Olafson, B. D., States, D. J., Swaminathan, S., & Karplus, M. (1983) *J. Comput. Chem.* (in press).

Cowan, D. O., & Drisko, R. L. (1976) *Elements of Organic Photochemistry*, Plenum Press, New York.

Dill, K., & Allerhand, A. (1979) *J. Am. Chem. Soc. 101*, 4376.

Dubin, S. B., Clark, N. A., & Benedek, G. B. (1971) *J. Chem. Phys. 54*, 5158.

Gelin, B. R., & Karplus, M. (1975) *Proc. Natl. Acad. Sci. U.S.A. 72*, 2002.

Gelin, B. R., & Karplus, M. (1979) *Biochemistry 18*, 1256.

Gill, T. J., McLaughlin, E. M., & Omenn, G. S. (1967) *Biopolymers 5*, 297.

Imoto, T., Forster, L. S., Rupley, J. A., & Tanaka, F. (1972a) *Proc. Natl. Acad. Sci. U.S.A. 69*, 1151.

Imoto, T., Johnson, L. N., North, A. C. T., Phillips, D. C., & Rupley, J. A. (1972b) *Enzymes, 3rd Ed. 7*, 665.

Jablonski, A. (1965) *Acta Phys. Pol. B 28*, 717.

Karplus, M., & McCammon, J. A. (1979) *Nature (London) 277*, 578.

Karplus, M., & McCammon, J. A. (1981) *CRC Crit. Rev. Biochem. 9*, 293.

Kasprzak, A., & Weber, G. (1982) *Biochemistry 21*, 5924.

Kinosita, K., Kawato, S., & Ikegami, A. (1977) *Biophys. J. 20*, 289.

Konev, S. V. (1967) *Fluorescence and Phosphorescence of Proteins and Nucleic Acids*, Plenum Press, New York.

Kurachi, K., Sieker, L. C., & Jensen, L. H. (1976) *J. Mol. Biol. 101*, 11.

Lakowicz, J. R., & Weber, G. (1973a) *Biochemistry 12*, 4161.

Lakowicz, J. R., & Weber, G. (1973b) *Biochemistry 12*, 4171–4179.

Lakowicz, J. R., & Weber, G. (1980) *Biophys. J. 32*, 591.

Lakowicz, J. R., Maliwal, B. P., Cherek, H., & Balter, A. (1983) *Biochemistry 22*, 174.

Levy, R. M., & Szabo, A. (1982) *J. Am. Chem. Soc. 104*, 2073.

Levy, R. M., Karplus, M., & McCammon, J. A. (1981a) *J. Am. Chem. Soc. 103*, 994.

Levy, R. M., Karplus, M., & Wolynes, P. G. (1981b) *J. Am. Chem. Soc. 103*, 5998.

Levy, R. M., Dobson, C., & Karplus, M. (1982) *Biophys. J. 39*, 107.

Lipari, G., & Szabo, A. (1980) *Biophys. J. 30*, 489.

Lipari, G., & Szabo, A. (1982) *J. Am. Chem. Soc. 104*, 4546.

Martin, J. L., Migus, A., Poyart, C., Lecarpentier, Y., Astier, R., & Antonetti, A. (1983) *Proc. Natl. Acad. Sci. U.S.A. 80*, 173.

McCammon, J. A., & Karplus, M. (1979) *Proc. Natl. Acad. Sci. U.S.A. 76*, 3585.

McCammon, J. A., Gelin, B. R., & Karplus, M. (1977) *Nature (London) 267*, 585.

McCammon, J. A., Wolynes, P. G., & Karplus, M. (1979) *Biochemistry 18*, 927.

Munro, I., Pecht, I., & Stryer, L. (1979) *Proc. Natl. Acad. Sci. U.S.A. 76*, 56.

Ribeiro, A., King, R., Restivo, C., & Jardetzky, O. (1980) *J. Am. Chem. Soc. 102*, 4040.

Richards, F. M. (1977) *Annu. Rev. Biophys. Bioeng. 6*, 151, 176.

Richarz, R., Nagayama, K., & Wuthrich, K. (1980) *Biochemistry 19*, 5189.

Robbins, R. J., Fleming, G. R., Beddard, G. S., Robinson, G. W., Thistlethwaite, P. J., & Wolfe, G. J. (1980) *J. Am. Chem. Soc. 102*, 6271.

Song, P.-S., & Kurtin, W. E. (1969) *J. Am. Chem. Soc. 91*, 4892.

Sternberg, M. J. E., Grace, D. E. P., & Phillips, D. C. (1979) *J. Mol. Biol. 130*, 231.

Sun, M., & Song, P.-S. (1977) *Photochem. Photobiol. 25*, 3.

Swaminathan, S., Ichiye, T., van Gunsteren, W. F., & Karplus, M. (1982) *Biochemistry 21*, 5230.

Tao, T. (1969) *Biopolymers 8*, 609.

Valeur, B., & Weber, G. (1977) *Photochem. Photobiol. 25*, 441.

van Gunsteren, W. F., & Karplus, M. (1982) *Biochemistry 21*, 2259.

Walker, M. S., Dedrar, T. W., & Lumry, R. (1967) *J. Chem. Phys. 47*, 1020.

Wallach, D. (1967) *J. Chem. Phys. 47*, 5258.

Weber, G. (1960a) *Biochem. J. 75*, 335.

Weber, G. (1960b) *Biochem. J. 75*, 345.

Wittebort, R. J., Rothgeb, M., Szabo, A., & Gurd, F. R. N. (1979) *Proc. Natl. Acad. Sci. U.S.A. 76*, 1059.

Yamamoto, Y., & Tanaka, J. (1972) *Bull. Chem. Soc. Jpn. 45*, 1362.